

## GODDARD SPACE FLIGHT CENTER

### Evaluation Report

"The information contained herein is presented for guidance of employees of the Goddard Space Flight Center. It may be altered, revised, or rescinded due to subsequent developments or additional test results. These changes could be communicated internally by other Goddard publications. Notice is hereby given that this document is distributed outside of Goddard as a courtesy only to other government agencies and contractors and is understood to be only advisory in nature. Neither the United States Government nor any person acting on behalf of the United States Government assumes any liability resulting from the use of the information contained herein."

Microcircuit (10)  
Mfr.: Analog Devices  
P/N: AD8138  
D/C: 0021

Malfunction Report

Purchase Specifications  
commercial

Incoming Inspected

Screening Specifications  
commercial

Project  
VCL  
System  
Parts testing  
Requester  
K.Sahu (562)  
Initiated Date  
10/01/00  
Investigator  
A.Teverovsky (562)

Approval for Distribution/Date

\_\_\_\_\_

## Background

Ten Analog Devices AD8138 commercial microcircuits intended for the VCL project were submitted to the GSFC Parts Analysis Laboratory for evaluation of their design, materials and potential risk for long term reliability.

## Part Description

The AD8138 is a low distortion differential ADC driver which operates similar to a differential op amp. The die is attached to the silver-plated copper lead frame using a silver epoxy and is interconnected to the leads with 1.2 mil gold wires. The part is encapsulated in a standard surface mount 8-lead plastic package (SOIC, type SO-8).

The part is designed using a high-speed complementary bipolar process, called XFCB (eXtra-Fast Complementary Bipolar). The XFCB is a variation of the SOI technology which employs bonded wafers with deep trenches to achieve full dielectric isolation. This process has been in production by Analog Devices for more than 6 years. This technology provides radiation hardening to the device and eliminates the possibility of latch-up failures.

An operating temperature range for the part is  $-40\text{ }^{\circ}\text{C}$  to  $+85\text{ }^{\circ}\text{C}$  and a storage temperature range  $-65\text{ }^{\circ}\text{C}$  to  $+150\text{ }^{\circ}\text{C}$ . The part can withstand lead temperature up to  $300\text{ }^{\circ}\text{C}$  for 10 seconds during soldering.

## **Analysis.**

### **1. External and Radiographic Examinations.**

External examination showed that the part had no package warping, cracks, voids, or foreign inclusions in the plastic encapsulant. No gaps were observed between the entry of the leads and the molding compound (MC). Figure 1 gives external views of the part.

Radiographic examination showed adequate wire bond dressing. The die-paddle and the leads had lead lock holes which enhanced a bond between the molding compound and the lead frame and increased moisture resistance of the part. Typical top and side X-ray views of the part are shown Figure 2.

### **2. Scanning Acoustic Microscopy.**

#### **2.1. Reflow simulation.**

Top sides of five parts were examined using an acoustic microscope (C-SAM mode with a 15 MHz transducer) before and after solder heat resistance simulation. This simulation was performed by immersing the parts in a solder pot at  $245 \pm 5\text{ }^{\circ}\text{C}$  for 5 seconds and then spray cleaned with isopropanol. This procedure was repeated three times.

External visual examination after solder pot simulation did not reveal any defects. C-SAM examination showed that delamination at the paddle-molding compound interface has developed in all parts (see Figure 3). No abnormalities at the die-molding compound interface or lead fingertips were noticed.

#### **2.2. Temperature cycling of DPA parts.**

Three parts after solder heat resistance simulation and two new parts were subjected to 100 temperature cycles between  $-65\text{ }^{\circ}\text{C}$  and  $+150\text{ }^{\circ}\text{C}$  with 15-minute dwell time. Acoustic images of the parts before and after temperature cycling are shown in Figure 4.

One new part withstood cycling without any changes (SN 10), however, in another part (SN 6), which had initially only small area of delamination at the paddle-MC interface, the area of delamination was significantly increased. Electrical testing of the parts at room temperature did not reveal any anomaly suggesting that the observed delaminations did not affect integrity of the parts.

All parts, which had been stressed by the solder pot test, had completely delaminated paddle-MC interface after temperature cycling. However, none of the parts had delamination at the die-MC interface.

### **2.3. Temperature cycling of flight parts.**

The above results suggest that the part might have problems when subjected to severe thermo-mechanical stresses. To ensure proper quality of the flight parts at normal conditions C-SAM examinations were performed on 30 AD8138 microcircuits before and after 20 temperature cycles  $-20^{\circ}\text{C} + 85^{\circ}\text{C}$ . The original purpose of this test was to pick the best candidates for space applications. The results showed that none of the parts had delaminations or any other defects neither before nor after the temperature cycling. This demonstrates that all parts in the flight lot have adequate thermo-mechanical integrity and robustness under normal conditions. Figure 5 shows typical acoustic images of the flight parts before and after temperature cycling.

### **3. Internal Examinations.**

Two samples were decapsulated in red fuming nitric acid and examined under high power optical microscope. No abnormalities in metallization patterning, glassivation integrity or wire bonding were observed. One die had a chip-out (see Figure 6) which did not affect the active area of the die and thus is not rejectable.

### **4. SEM inspection of metallization.**

The quality of metallization was inspected in two samples per MIL-STD-883D, Method 2018 (see Figures 7 to 9). The part has two aluminum metallization levels. The first level employs a thin Ti/W barrier layer (see Figure 10). No patterning or step coverage problems were found in either the top or the bottom metallization layers. Some misalignment in the level 1-to-level 2 contact windows (see Figure 9) did not exceed the acceptable level.

### **5. Package-level Cross Sectional Examinations.**

Two samples were cross-sectioned at several planes to examine interfaces between the molding compound and the die assembly. Figure 11 shows an overall view of the package cross section and Figures 12 and 13 show close-up views of different interfaces in the part.

The molding compound had no internal cracks or voids and formed intimate contacts to all internal surfaces (die, wires, and lead frame). No delaminations between the glassivation and the molding compound were observed.

The lead frame was made of copper of approximately  $200\text{ }\mu\text{m}$  thick. Fingertips of the leads and the top and the sidewall of the die paddle were locally spot-plated with silver (approximately  $5\text{ }\mu\text{m}$  thick). External parts of the lead frame were tinned.

The die was mounted to the lead frame base with a thin layer of silver epoxy. The adhesive and silver filler were uniformly distributed along the die-paddle interface.

Ball bond cross sectioning showed the formation of an adequate Au/Al intermetallic layer of 2 - 3  $\mu\text{m}$  in thickness (see Figure 14). In many cases a large proportion of the bonded area had the aluminum film completely consumed during intermetallic formation. Although similar condition is

typical for many microcircuits encapsulated in plastics, its effect on the long-term reliability of the part requires additional analysis.

## **Conclusions.**

1. The Analog Devices AD8138 commercial plastic encapsulated microcircuit is designed using a variation of SOI technology which provides radiation hardening to the part and eliminates the possibility of latch-up failures.
2. The die manufacturing was satisfactory. No rejectable defects were found in the glassivation, and the metallization systems.
3. The wire bonding exhibited normal alignment, dressing, and common for plastic encapsulated micircuits Au/Al intermetallic at the die contact pads.
4. Cross sectioning indicated good integrity of the part. The molding compound formed intimate contact to the leads and to all elements of the die-lead frame assembly.
5. SMT simulation (solder pot resistance) and temperature cycling (in the range  $-65^{\circ}\text{C}$  to  $+150^{\circ}\text{C}$ ) indicated that the part might have problems related to the formation of delaminatons at the lead frame/paddle – molding compound interface when subjected to severe thermo-mechanical stresses. However, at common for the plastic parts temperature cycling range of  $-20^{\circ}\text{C}$  to  $+85^{\circ}\text{C}$  no defects were observed suggesting that these parts most likely will not have any reliability problems operating under normal conditions.

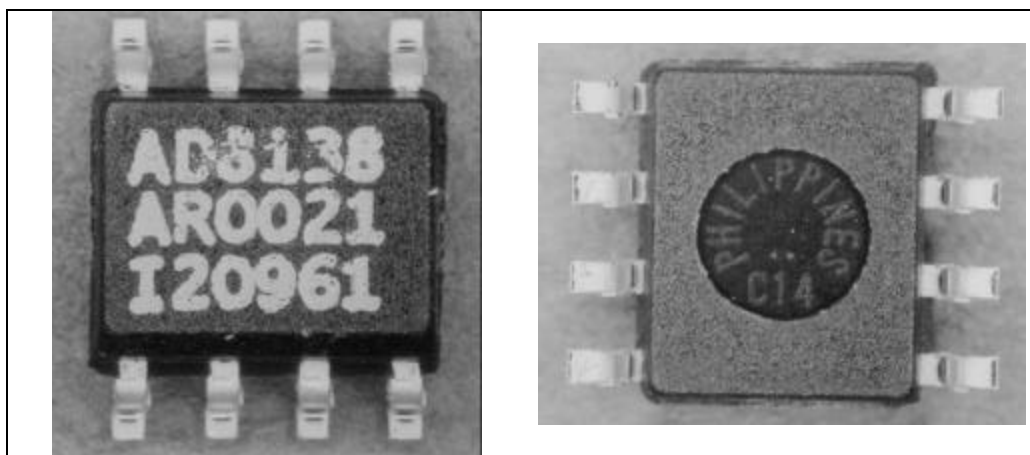


Figure 1. Top and bottom views of the part.

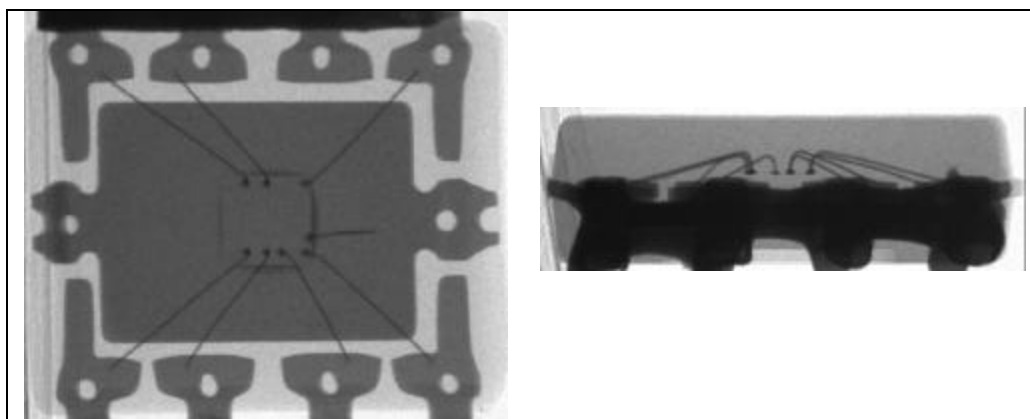


Figure 2. Typical top and side radiographic views of the part showing adequate lead frame design, wire dressing and layout.

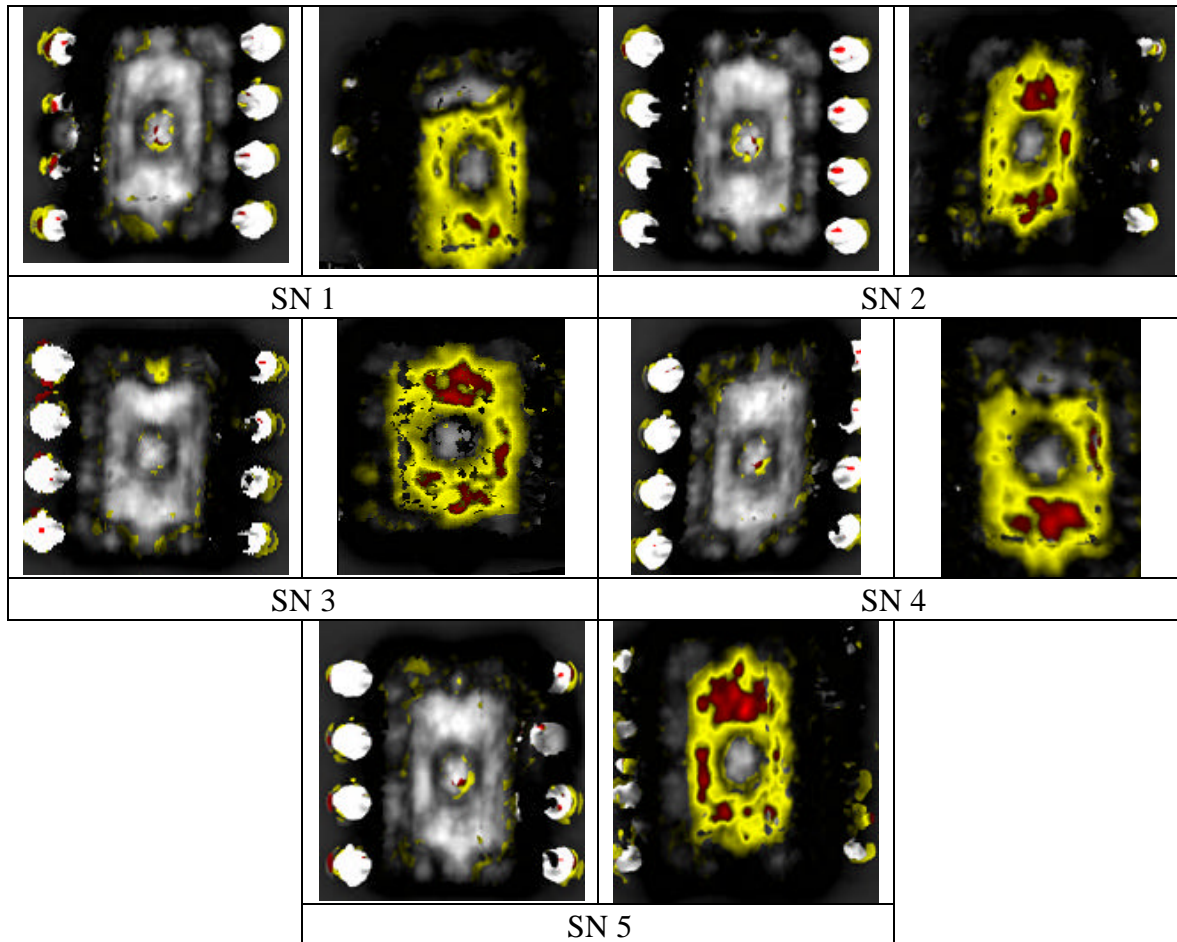


Figure 3. Analog Devices AD8138 acoustic images before (left) and after (right) solder pot test.  
Top side.

( $f = 15$  MHz,  $Z = 21.4$  us, pos. 0.347, wind. 0.35)

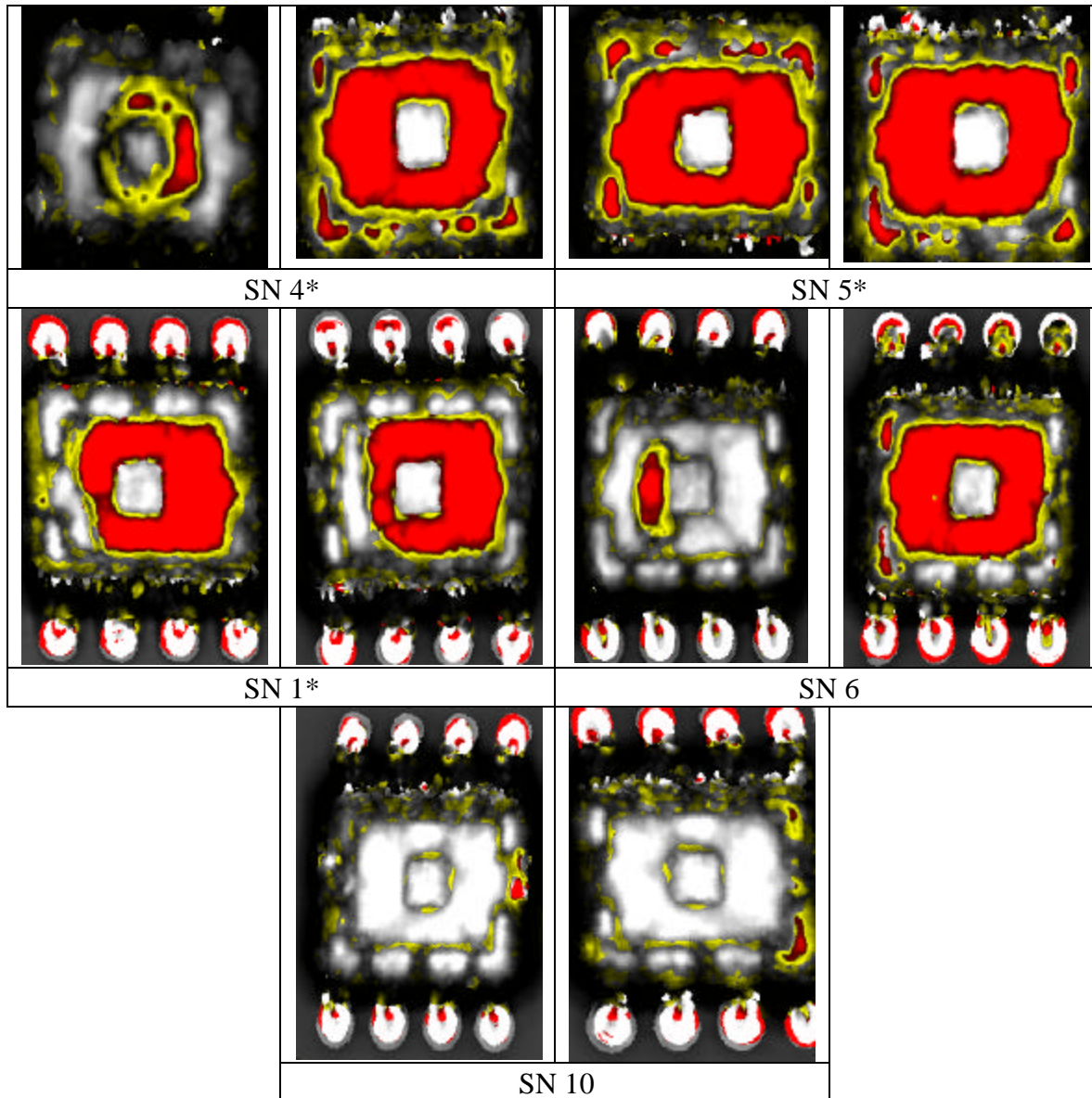


Figure 4. Acoustic images before (left) and after (right) 100 temperature cycles between  $-65^{\circ}\text{C}$  and  $+150^{\circ}\text{C}$ . Top side. Samples 1, 4, and 5 were subjected to the solder pot test before temperature cycling.

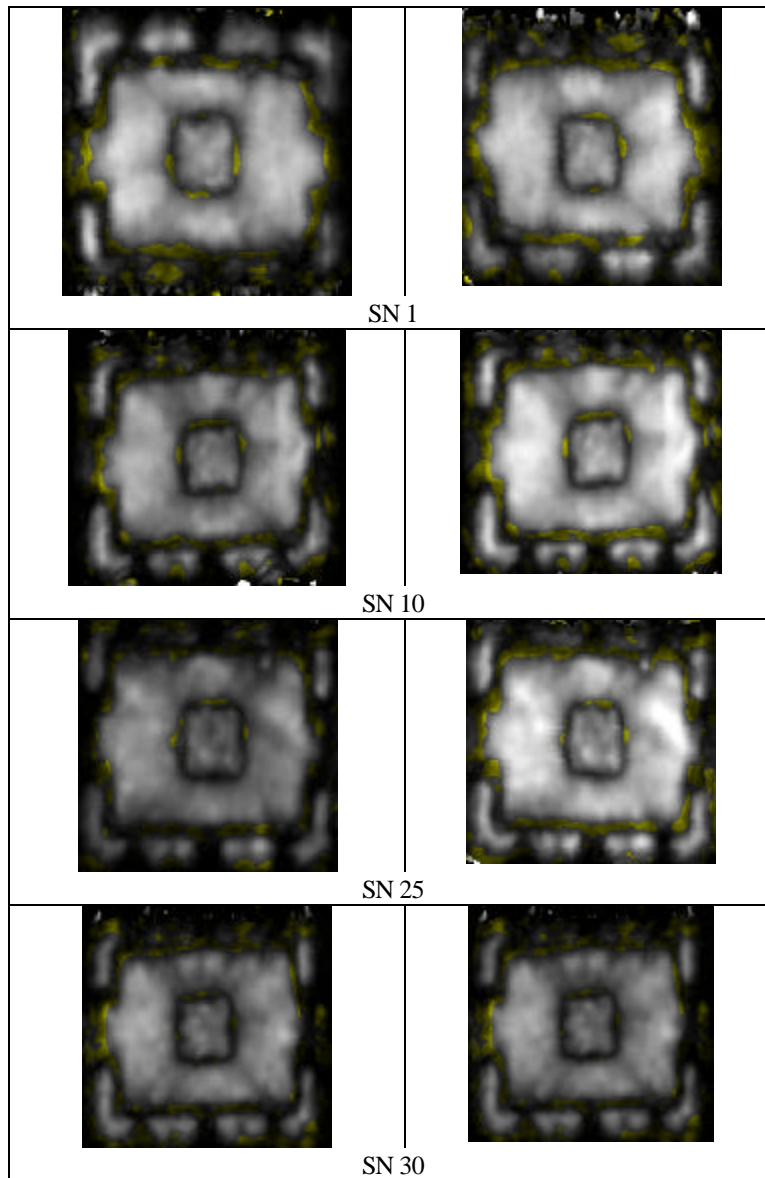


Figure 5. Typical acoustic images before (left) and after (right) 20 TC -20 °C to +85 °C. Top views.



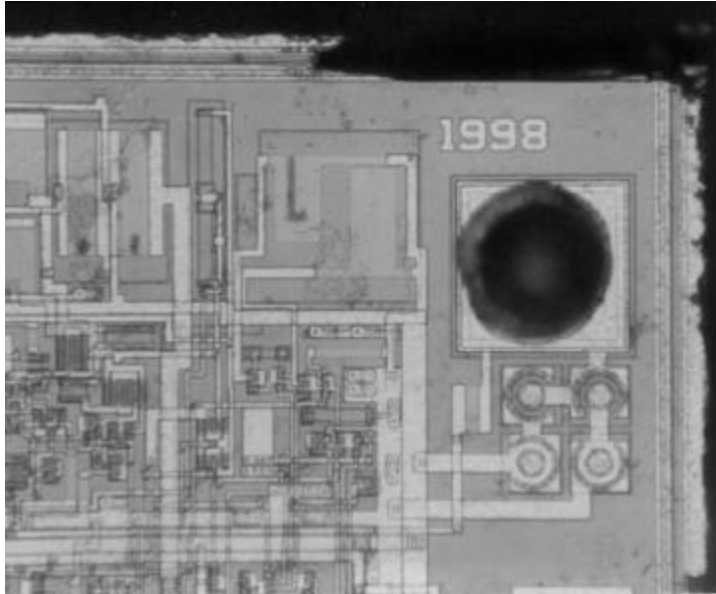


Figure 6. Chip-out in this die did not affect the active area of the microcircuit. (200X)

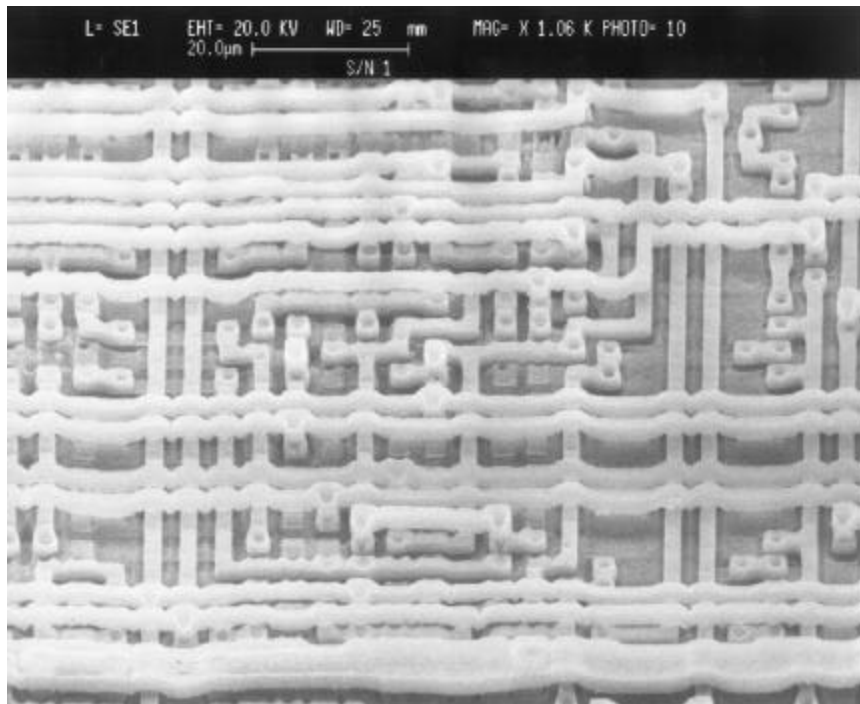


Figure 7. Overall SEM view of the die metallization. (1000X)

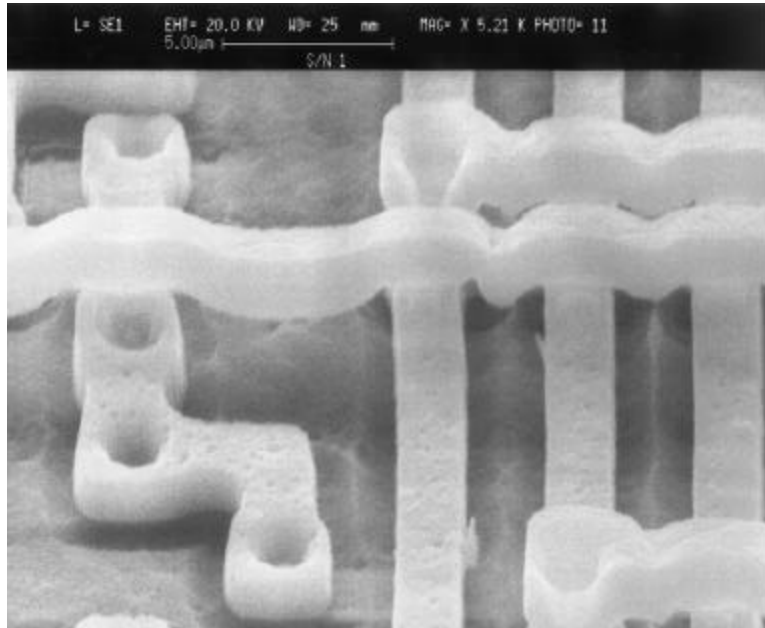


Figure 8. Close-up SEM view of the metallization. (5100X)

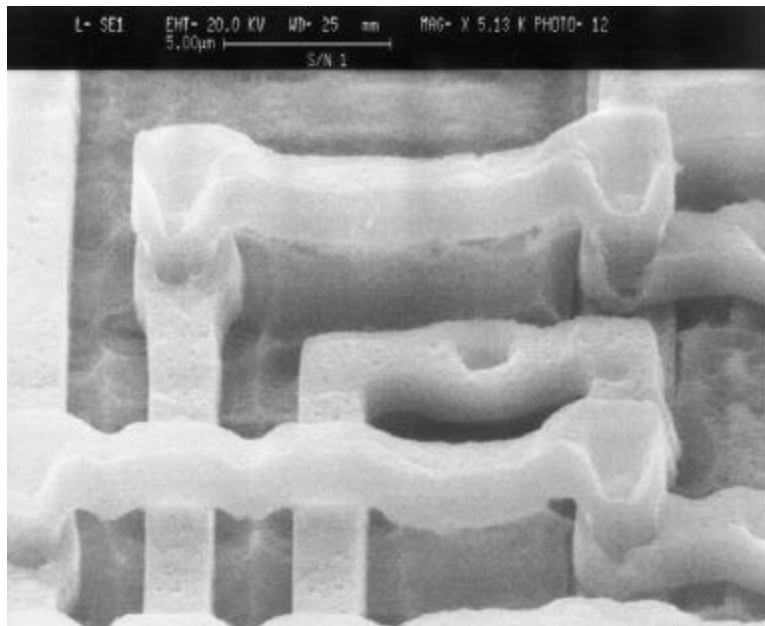


Figure 9. Misalignment in the level 1-to-level 2 contact windows did not exceed the acceptable level.

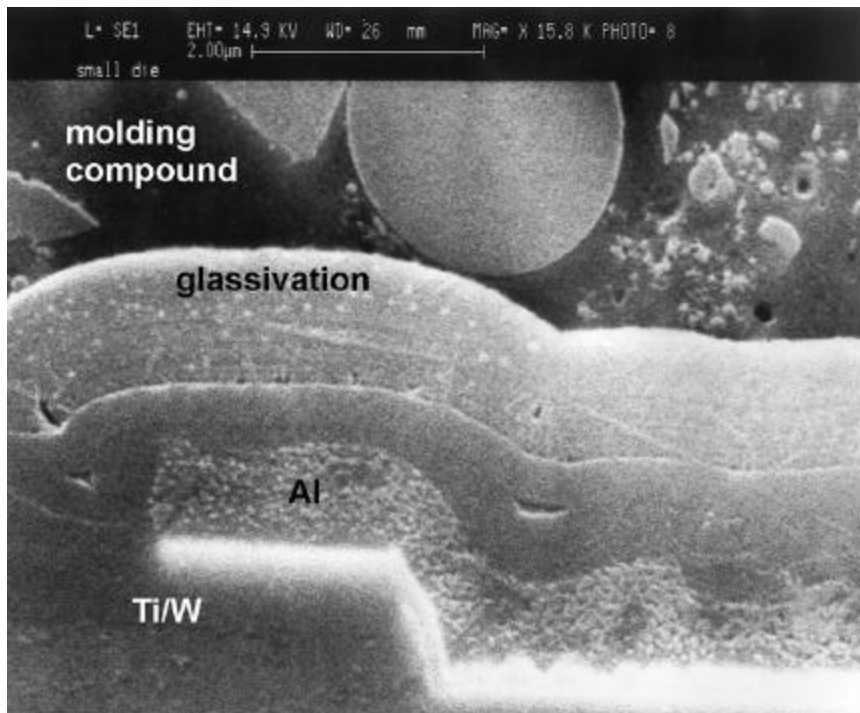


Figure 10. SEM view of the die cross section showing Ti/W barrier layer. Note also an intimate contact between the molding compound and the glassivation layer.

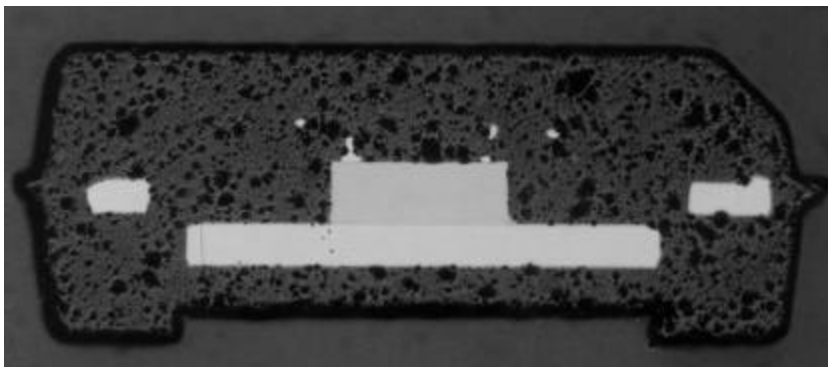


Figure 11. An overall view of the package cross section.

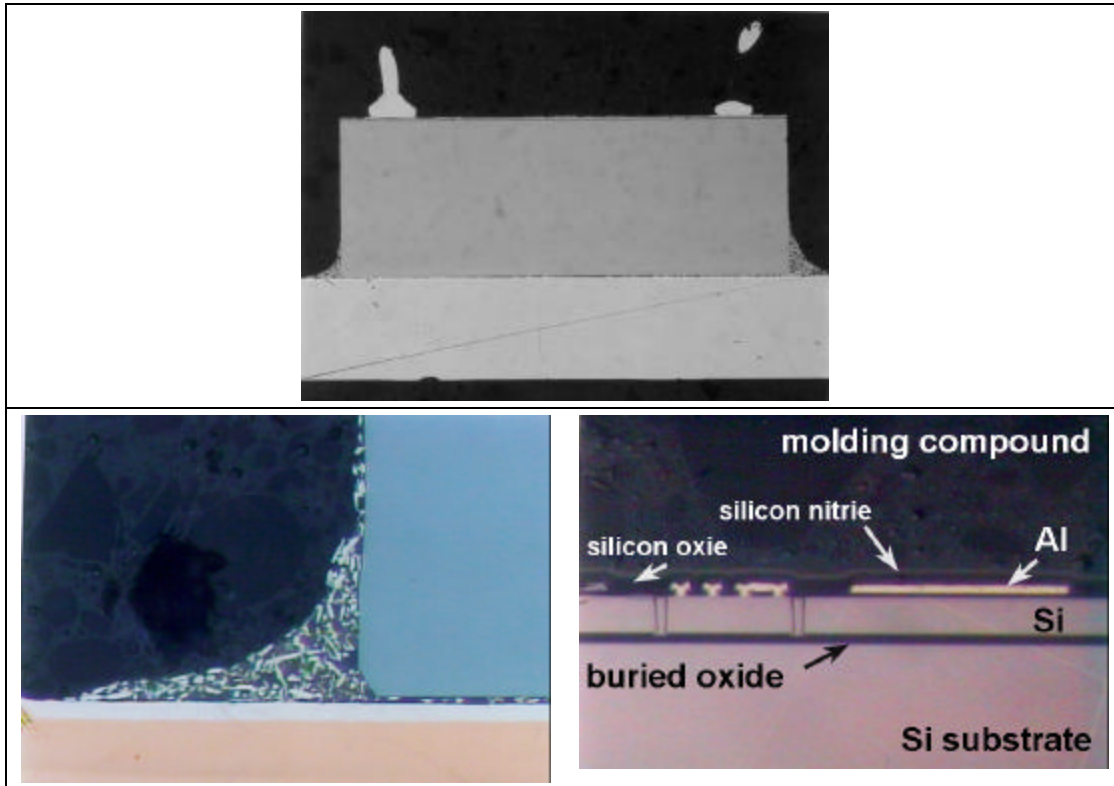


Figure 12. Die cross section (a) and close-up of the die attachment (b) and die surface (c).

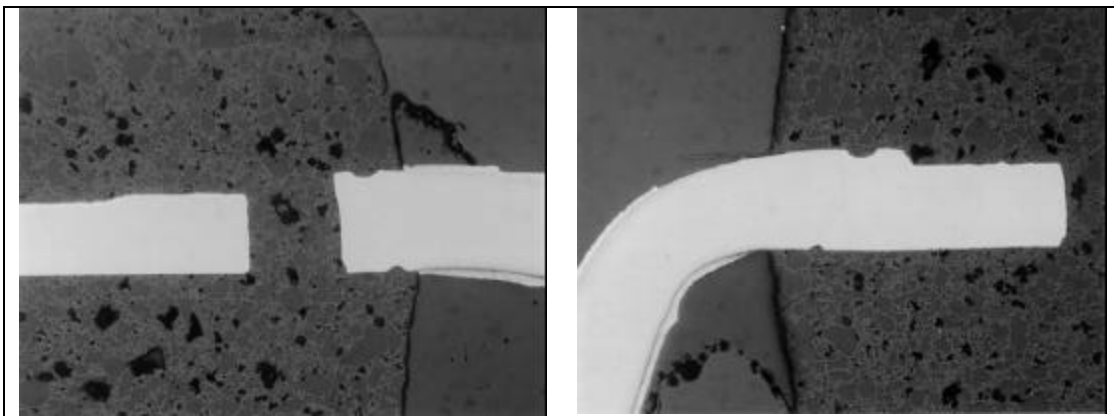


Figure 13. Cross-section of the lead entries showing intimate contact at the lead-MC interface.  
(100X)

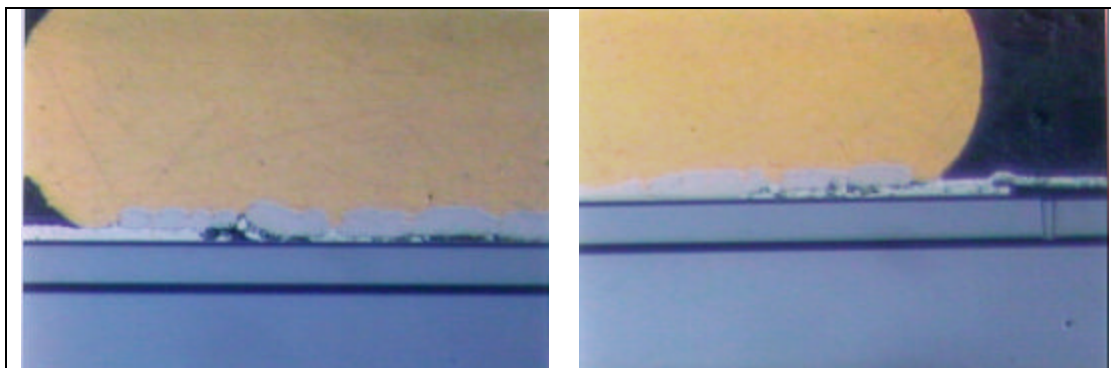


Figure 14. Cross-section of the wire bonds showing adequate Au/Al intermetallic formation at the edges of the bonds and aluminum thinning at the center. (1000X)